Improvement in Output Characteristics Using a Resonator and Passive Rectifiers in Vibration Generators

Masataka Minami

***Abstract*—Energy harvesting has attracted increased attention recently. Energy sources are present all around us, such as, mechanical vibrations, stress, strain, waste heat, sunlight or room light, electromagnetic rays, and chemical or biological sources. Vibration generators based on piezoelectric elements have been highlighted as low-power sources; however, their output power is very low, around the milliwatt or microwatt level, and thus, improving their performance is necessary to make the generated power usable. This paper investigates the use of passive devices to improve output characteristics of the vibration generators. The proposed circuits are a resonator and a passive rectifier. The proposed resonator consists of a parallel inductor and capacitor for LC resonance. The LC resonance equivalently reduces the internal capacitor of the piezoelectric elements. As a result, the output voltage and power are increased compared with that of conventional circuits. In addition, a boost-type current-improving passive rectifier is applied as the passive rectifier. The validity of the proposed circuit is numerically and experimentally verified.**

***Index Terms*—Boost-type current-improving passive rectifier, energy harvesting, LC resonance, passive rectifiers, piezoelectric elements, vibration generators.**

I. Introduction

ENERGY-HARVESTING systems have attracted increased attention recently [1]. The application of the system determines what energy sources are available in the environment to power it [2]. Ambient energy sources include vibration, solar, and thermal energies [3]. The system is expected to become practical application [2]. This research focuses on vibration generators based on piezoelectric elements. The vibration generators convert vibration energy into electric energy [4], [5], in way similar to that of solar generators and electromagnetic generators [6]. As the vibration generators provide very low power around the milliwatt or microwatt level, vibration generators cannot maintain large power outputs [7], [8]. Therefore, performance improvement of the vibration generators is required for utilization.

Manuscript received September 5, 2018; revised October 30, 2018; accepted December 2, 2018. Date of publication December 5, 2018; date of current version May 22, 2019. Recommended for publication by Associate Editor M. Vitelli.

The author is with the Department of Electrical Engineering, Kobe City College of Technology, Kobe 651-2194, Japan (e-mail:

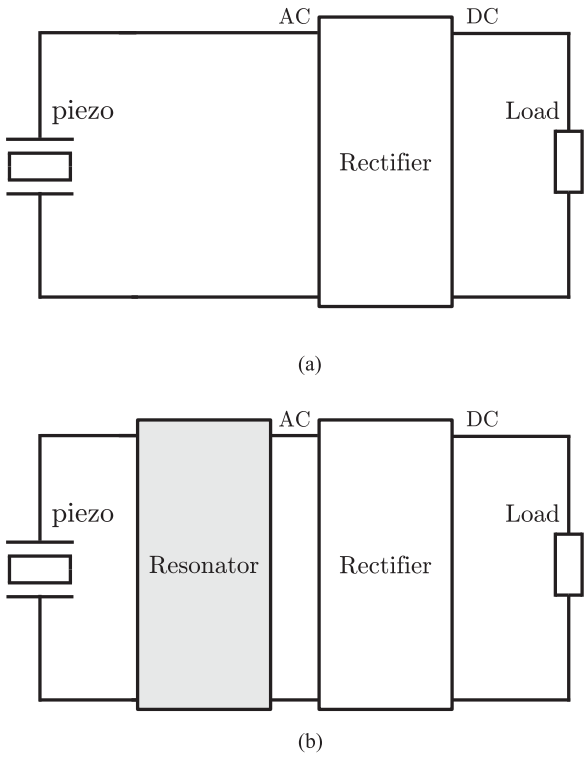

Fig. 1. Circuit structure of the piezoelectric elements used in the vibration generator. (a) Conventional approach. (b) Proposed approach.

In this paper, two approaches to improve performance are proposed: LC resonance and a passive rectifier. The first approach uses the resonator. Many researchers have focused on mechanical resonance to improve the performance of vibration generators. However, electrical resonance was not generally used in vibration generators. Costanzo *et al.* [9] applied the additional non-dissipative component for the resonant electromagnetic vibration energy harvesters. This paper proposes the similar method for the piezoelectric element in the vibration generators. Fig. 1 shows a vibration generator and its interface circuit. Here, Fig. 1(a) is the conventional system. The piezoelectric element connects to the rectifier to convert dc power. Then, the rectifier provides dc power to the load. This paper proposes the resonator circuit for an LC resonance. The resonator aims to increase the output power from the piezoelectric element. The LC resonance equivalently reduces the inter-

Fig. 2. Size and structure of the piezoelectric element used in this paper.

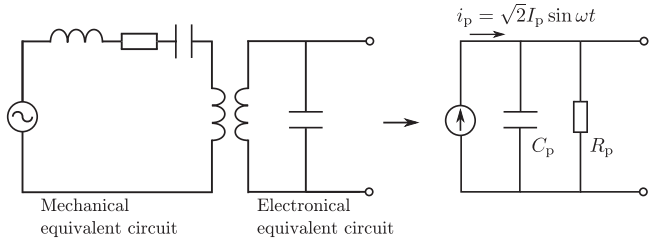

Fig. 3. Equivalent circuit of piezoelectric elements [16].

nal capacitance of piezoelectric elements. As a result, the output power is increased compared with that of the conventional circuit [10].

The second approach uses a passive rectifier. As the output power of the piezoelectric element is ac power, the rectifier is needed for applications. Kwon and Rincon-Mora [11] suggested a rectifier-free circuit for piezoelectric energy harvesting. The circuit consists of two active switches, an inductor, and two diodes. Ramadass and Chandrakasan [12] used a bias-flip rectifier with an inductor. Peters *et al.* [13] proposed a two-stage concept including passive stage and one active diode. However, the rectifier including an active switch needs the driving energy for switching. This paper focuses on the all-passive rectifier for the piezoelectric energy-harvesting system. Thus, we numerically compared the all-passive rectifiers: the diode bridge (DB) rectifier, the voltage doubler (VD) rectifier, and the boost-type current-improving (BC) rectifier. As a result, we found that the BC rectifier matches the vibration generators about the output characteristics. Therefore, this rectifier is adopted in this paper.

Finally, it is numerically and experimentally clarified that the proposed resonator and rectifier improves the output characteristics in vibration generators.

II. Equivalent Circuit of Piezoelectric Elements

Fig. 2 shows the size and structure of the piezoelectric element used in this paper. The right-hand side of the piezoelectric element is clamped and vibrated by a vibration source. On the other side of the piezoelectric element, the mass is tipped for the mechanical resonance to increase the amplitude.

The target application is the vibration of engines, such as in a motor vehicle [14]. Thus, the vibration frequency is around 7000 r/min. In this paper, the frequency is assumed constant and set to 120 Hz. The problem of frequency change is left for future work. The specific application is a main or auxiliary power supply for the sensors and control units in the motor vehicle. The method of this paper has the issue about the circuit size. The improvement of the size leaves for future work. This paper just proposes the improvement in the output characteristics and verifies the method.

Piezoelectric elements convert vibration energy into electric energy [15]. The piezoelectric elements are expressed as shown in Fig. 3 (see [16]). The vibration energy and the piezoelectric ceramic are expressed in the ac current source and internal impedance as a capacitor and a resistor [16]. In this paper, the C_p means an equivalent capacitor. The capacity of the power generation is included in the current source of Fig. 3. Therefore, the capacity of the power generation does not decrease when the C_p decreases.

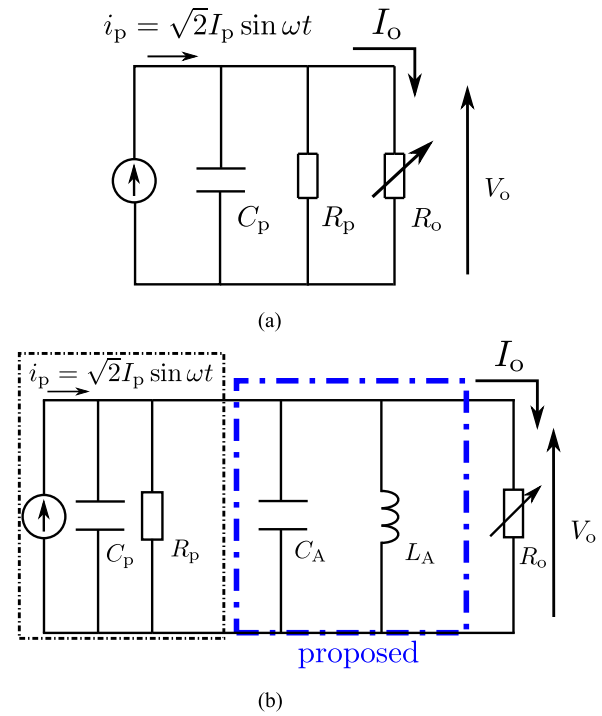

Fig. 4. Vibration generators, shown in the equivalent circuit, connect with the resistor R_o for the estimation of ac output characteristics. In the proposed circuit, the parallel inductor L_A and capacitor C_A connect with the vibration generators. (a) Conventional ac circuit. (b) Proposed ac circuit.

III. Resonator

A. Principle

Fig. 4(a) represents Fig. 3 connected with the load R_o. The output current I_o and the output power P_o in Fig. 4(a) are expressed as follows:

$$I_o = \sqrt{I_p^2 - (\omega C_p)^2 V_o^2} - \frac{V_o}{R_p} \tag{1}$$

$$P_o = V_o I_o = V_o \sqrt{I_p^2 - (\omega C_p)^2 V_o^2} - \frac{V_o^2}{R_p} \tag{2}$$

where V_o denotes the output voltage. As the internal resistor R_p is large enough, the R_p is ignored. At that time, the maximum output power $P_o^{\max}$ becomes $I_p^2/2\omega C_p$ when the load $R_o = 1/\omega C_p$ matches the impedance. The output power P_o

TABLE I
PARAMETERS OF THE PIEZOELECTRIC ELEMENTS AND THE RESONATOR

$I_{\rm p} = 9.2$ mA	$\omega = 2\pi \times 120$ rad/s
$C_{\rm p} = 1.06$ μF	$R_{\rm p} = 2.8$ kΩ
$L_{\rm A} = 816.3$ mH	$R_{\rm A} = 56.4$ Ω
$C_{\rm A} = 1$ μF	

depends on the internal capacitance $C_{\rm p}$ from this result. Therefore, the LC resonance equivalently reduces the internal capacitance $C_{\rm p}$. Fig. 4(b) represents the proposed circuit using the LC resonance. A parallel inductor $L_{\rm A}$ and capacitor $C_{\rm A}$ connect with the vibration generators. The parallel inductor $L_{\rm A}$ and capacitor $C_{\rm A}$ resonate with the internal capacitor $C_{\rm p}$. In the ideal viewpoint, the parallel capacitor $C_{\rm A}$ does not require the LC resonance. However, in practice, the parallel capacitor $C_{\rm A}$ plays an important role in the circuit. The value of the inductor is much less accurate. The parallel capacitor $C_{\rm A}$ adjusts the LC resonant frequency. In addition, the parallel inductor $L_{\rm A}$ becomes a large value and a huge volume when the only parallel inductor $L_{\rm A}$ neutralizes the internal capacitance $C_{\rm p}$. Therefore, the parallel capacitor $C_{\rm A}$ reduces the value of the parallel inductor $L_{\rm A}$.

The LC resonance equivalently enables a reduction in the internal capacitance $C_{\rm p}$. The output current of Fig. 4(b) is expressed as follows: [10]

$$I_{\rm o} = \sqrt{I_{\rm p}^2 - \left\{\omega(C_{\rm p}+C_{\rm A}) - \frac{\omega L_{\rm A}}{R_{\rm A}^2 + (\omega L_{\rm A})^2}\right\}^2 V_{\rm o}^2} - \left(\frac{1}{R_{\rm p}} + \frac{R_{\rm A}}{R_{\rm A}^2 + (\omega L_{\rm A})^2}\right) V_{\rm o} \quad (3)$$

where the resistor $R_{\rm A}$ denotes the series resistor of the parallel inductor $L_{\rm A}$. When the internal resistor $R_{\rm p}$ and the series resistor $R_{\rm A}$ is ignored

$$I_{\rm o} = \sqrt{I_{\rm p}^2 - \left\{\omega(C_{\rm p}+C_{\rm A}) - \frac{1}{\omega L_{\rm A}}\right\}^2 V_{\rm o}^2}. \quad (4)$$

The resonant condition is $\omega^2 L_{\rm A}(C_{\rm p}+C_{\rm A}) = 1$.

B. Setting

Table I lists the parameters of the vibration generators and the resonator. Here, we explain each parameter. First, the value of the parallel inductor $L_{\rm A}$ is designed. As the parallel inductor $L_{\rm A}$ neutralizes the internal capacitance $C_{\rm p}$ and the parallel capacitor $C_{\rm A}$, the following equation holds:

$$\omega = \frac{1}{\sqrt{L_{\rm A}(C_{\rm p}+C_{\rm A})}} \quad (5)$$

$$L_{\rm A} = \frac{1}{\omega^2(C_{\rm p}+C_{\rm A})} \approx 853\ {\rm mH} \quad (6)$$

where the series resistor $R_{\rm A}$ is ignored. The inductor $L_{\rm A}$ is measured by an *LCR* hi-tester 3532-50: $L_{\rm A} = 816.3$ mH and $R_{\rm A} = 56.4$ Ω. Fig. 5 shows the inductor $L_{\rm A}$. The volume is 1.17 kg. Here, the capacitor $C_{\rm A}$ is fixed from the preliminary experiment. The preliminary experiment changes the parameter $C_{\rm A}$ every 0.1 μF. The parameter $C_{\rm A}$ is chosen when the output power becomes maximum value. Second, the parameters of the piezoelectric elements for vibration generators are the ac current amplitude $I_{\rm p}$ and the internal capacitor $C_{\rm p}$ and resistor $R_{\rm p}$. Those parameters are measured from the result of a preliminary experiment.

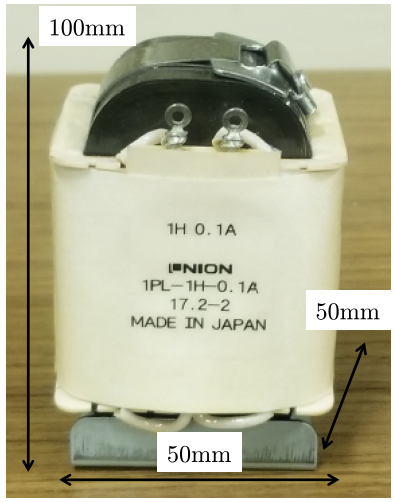

Fig. 5. Photograph of inductor for resonator.

C. Results

Fig. 6(a) and (b) describes the I–V and P–V ac characteristics of the ideal equations and the numerical results [10]. As the inductor $L_{\rm A}$ and the parallel capacitor $C_{\rm A}$ neutralize the internal capacitor $C_{\rm p}$, the output current $I_{\rm o}$ increases, as shown in Fig. 6(a). In addition, the maximum output power of the proposed circuit is higher than the conventional circuit in Fig. 6(b).

In Fig. 6(a) from 0 to 4 V, the conventional and proposed results are similar. Compared with (1) and (3), the reasons are two. One is the low voltage. In this range, the second terms in the root of the equations have a low impact on the output current drop since the output voltage $V_{\rm O}$ is low. The other is the series resistor $R_{\rm A}$ of the inductor $L_{\rm A}$. Equation (3) has the term included the series resistor $R_{\rm A}$ of the inductor $L_{\rm A}$. This term drops the output current $I_{\rm O}$.

IV. PASSIVE RECTIFIERS

As the output power is generally used as dc power, rectifiers are necessary to convert the output power of the piezoelectric elements into dc power. The various rectifiers, such as those shown in Fig. 7(a) and (b), are widely used in many systems [17], [18]. Fig. 7(a) describes a DB and Fig. 7(b) describes a VD. The output voltage of the DB is lower than the VD. In contrast, the output power of the DB is larger than the VD. These circuits are well known to have such problems. Fujiwara and Nomura [19] proposed a novel passive rectifier, as shown in Fig. 7(c). The rectifier improves the output power and voltage by using a diode rectifier with improved input current waveform [19].

In this section, DB, VD, and BC are numerically compared with regards to the output characteristics. The operations of the rectifiers are expressed in every mode.

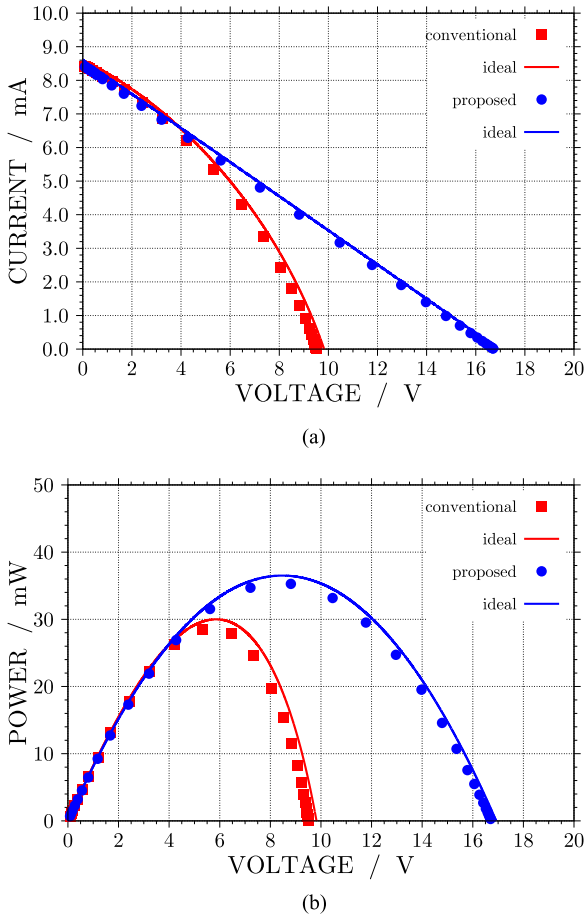

Fig. 6. I–V and P–V ac characteristics of the ideal equations and the numerical results [10]. (a) I–V. (b) P–V.

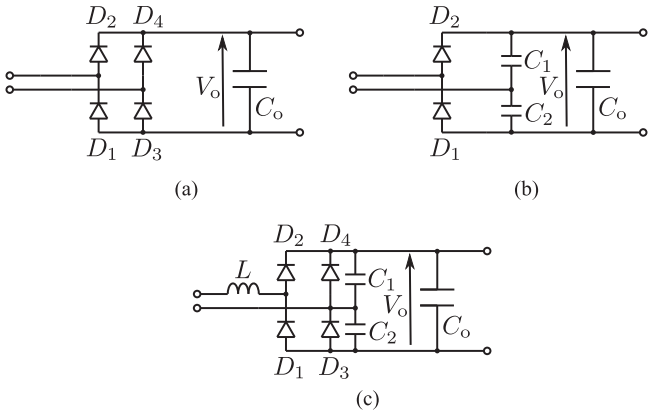

Fig. 7. Various rectifier circuits using passive devices. (a) Diode bridge rectifier [17], [18]. (b) Voltage doubler rectifier [17]. (c) Boost-type current-improving passive rectifier [19].

A. Numerical Conditions and Parameters

A circuit simulator called LTspice IV was used for the numerical analysis. Table II lists the parameters of the rectifiers. The parameters are set by the results of preliminary experiments. The resistor $R_{\rm L}$ denotes the series resistor of the inductor L in the rectifier. The diodes of the rectifiers are Schottky barrier diodes 1N5818. The vibration generator in Fig. 3 connects to every rectifier in Fig. 7. Here, to compare the three rectifiers, the resonator proposed in Section III is not used in this section.

TABLE II
PARAMETERS OF THE RECTIFIERS

$L = 150$ mH	$R_{\rm L} = 10.4\ \Omega$
$C_1 = C_2 = 0.33\ \mu$F	$C_{\rm o} = 22\ \mu$F

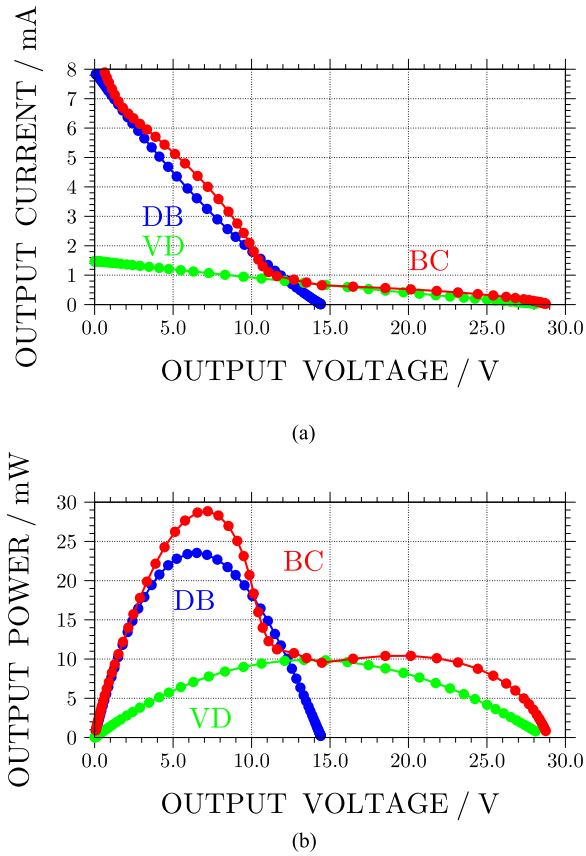

Fig. 8. I–V and P–V output characteristics of the DB, VD, and BC. (a) I–V. (b) P–V.

B. I–V and P–V Characteristics

Fig. 8 represents the numerical results of the three rectifier circuits. Fig. 8(a) and (b) describes I–V and P–V characteristics. First, in Fig. 8, the output voltage of the DB is lower than that of the VD. On the other hand, the output power of the DB is larger than that of the VD in Fig. 8(b). The features of the DB and VD are implied. Second, the BC is compared with the DB and VD. The maximum output voltage of the BC is as high as that of the VD. Furthermore, the maximum output power of the BC is larger than that of the DB. Therefore, the BC improves the output voltage and power.

C. Operation Modes

In this section, the operation modes of the rectifier circuits are divided and verified.

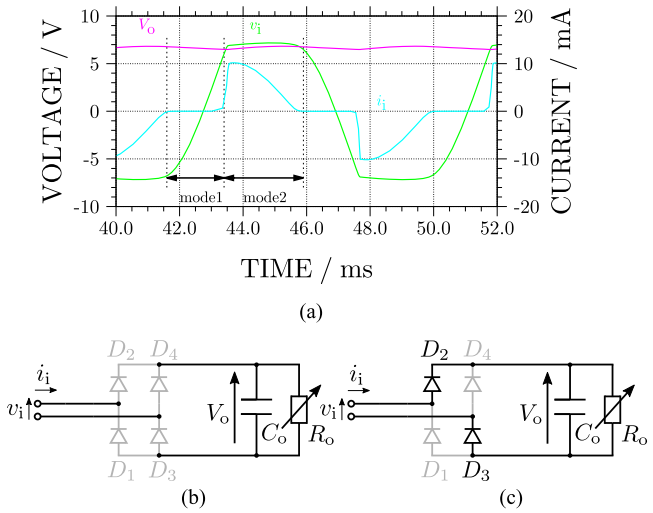

Fig. 9. Time waveforms and the operation modes of the circuit with the diode bridge rectifier. (a) $V_o = 6.5$ V. (b) Mode 1. (c) Mode 2.

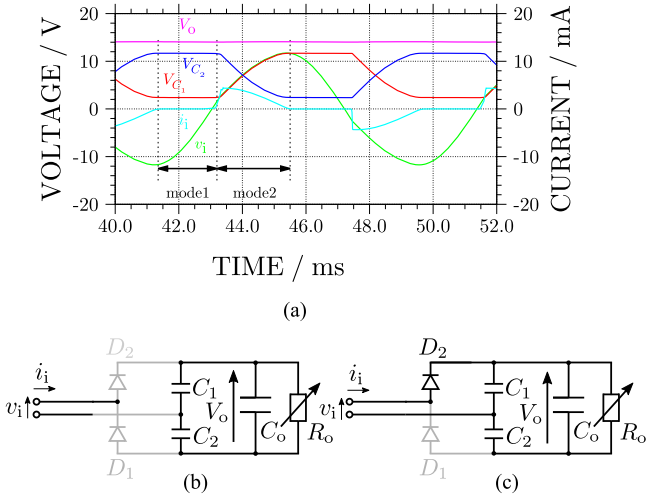

Fig. 10. Time waveforms and the operation modes of the circuit with the voltage doubler rectifier. (a) $V_o = 14$ V. (b) Mode 1. (c) Mode 2.

In the case of the DB, Fig. 9(a) represents the time waveforms and Fig. 9(b) and (c) illustrates the operation modes of Fig. 9(a). In mode 1, all diodes are turned OFF. Therefore, the input current i_i does not flow. After that, mode 1 shifts to mode 2. In mode 2, the diodes D_2 and D_3 conduct. Therefore, the input current i_i flows to the load R_o.

In the case of the VD, Fig. 10(a) represents the time waveforms and Fig. 10(b) and (c) illustrates the operation modes of Fig. 10(a). As each capacitance of C_1 and C_2 is small in this paper, each voltage of the capacitors fluctuates. In mode 1, all the diodes are turned OFF. Therefore, the input current i_i does not flow. When mode 1 shifts to mode 2, the diode D_2 conducts. Therefore, the input current i_i flows to C_1 and C_2.

The BC has two distinctive waveform patterns. In the case of the BC in the low-voltage region ($V_o = 7$ V), Fig. 11(a) represents the time waveforms and Fig. 11(b) and (c) illustrates the operation modes of Fig. 11(a). In the low-voltage region, the BC has three operation modes. In mode 1, only the diode

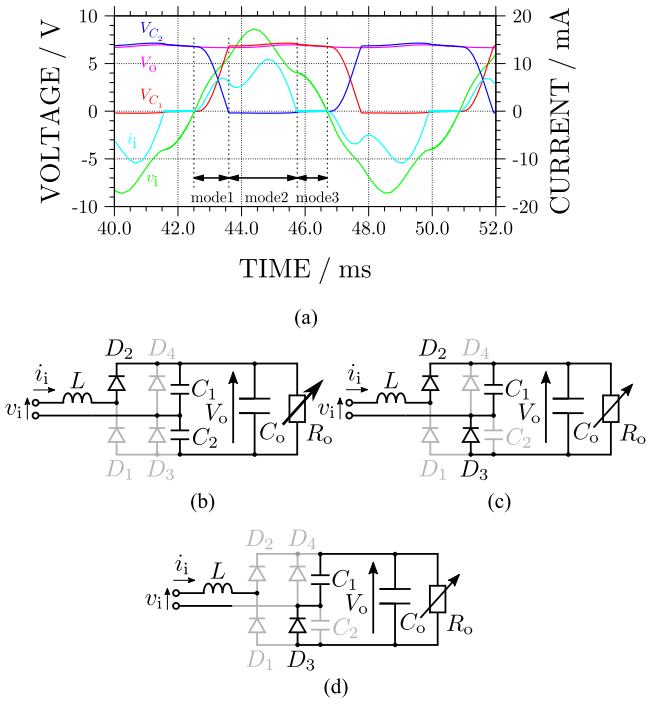

Fig. 11. Time waveforms and the operation modes of the BC in the low-voltage region. (a) $V_o = 7$ V. (b) Mode 1. (c) Mode 2. (d) Mode 3.

D_2 conducts. Therefore, the charging current flows to C_1, and the discharging current flows through the load R_o to C_2. When the capacitors finish charging and discharging, mode 1 shifts to mode 2. In mode 2, the diodes D_2 and D_3 conduct. Therefore, the input current i_i flows to the load R_o. First, because the inductor stores the energy, the input current i_i continues to flow. However, when the input voltage v_i is lower than the output voltage V_o, the input current i_i decreases. Second, when the input voltage v_i is higher than the output voltage V_o, the input current i_i increases. Finally, when the input voltage v_i is lower than the output voltage V_o, the input current i_i decreases again. As the input current i_i becomes zero, mode 2 shifts to mode 3. In mode 3, the diode D_3 conducts and D_2 does not conduct. As the input side does not supply power, C_o and C_1 supply power to the load R_o. Here, we focus on the interval when the input current i_i is flowing. In Fig. 9(a), the input current i_i only flows in mode 2. On the other hand, in Fig. 11(a), the input current i_i flows in mode 1 and mode 2. In addition, the output voltage of Fig. 11(a) is higher than Fig. 9(a). For these reasons, in the low-voltage region, the output power of the BC is larger than that of the DB.

In the case of the BC in the high-voltage region ($V_o = 20$ V), Fig. 12(a) represents the time waveforms and Fig. 12(b) and (c) illustrates the operation modes of Fig. 12(a). In the high-voltage region, the BC has the two operation modes. In mode 1, all the diodes are turned OFF. Therefore, the input current i_i does not flow. In mode 2, the diode D_2 conducts. At that time, the charging current flows to C_1, and the discharging current flows through the load R_o to C_2. In the high-voltage region, the operation modes of the BC are similar to those of the VD. In addition, the input current i_i increases by the inductor. Therefore,

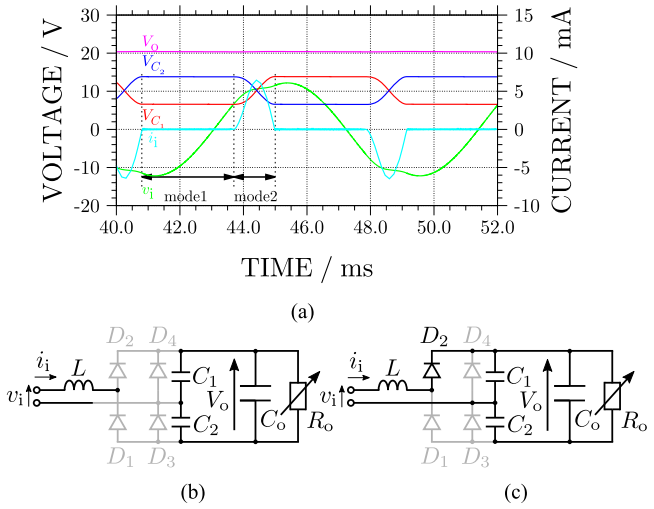

Fig. 12. Time waveforms and the operation modes of the BC in the high-voltage region. (a) $V_o = 20$ V. (b) Mode 1. (c) Mode 2.

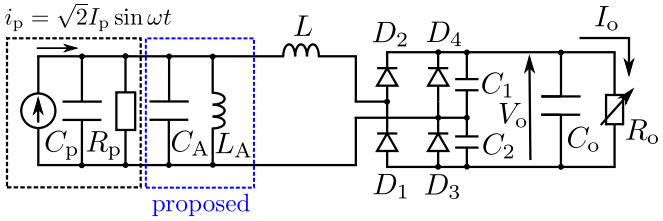

Fig. 13. Proposed circuit with the boost-type current-improving passive rectifier.

in the high-voltage region, the maximum output voltage of the BC is higher than that of the DB, and the output power of the BC is larger than that of the VD. For these reasons, the BC improves the output voltage and power.

This section shows and compares the qualitative analysis about DB, VD, and BC. The quantitative analysis will give more insight. However, these rectifiers include the diode devices, which are nonlinear devices. Hence, the quantitative analysis is very difficult and is left for the future work.

V. Verification of the Proposed Circuit

Fig. 13 shows the proposed circuit with the BC. The vibration source and system configuration are explained. Fig. 14 shows a photograph of the system. The ten piezoelectric elements for vibration generators connect electrically in parallel and mechanically in a circular pattern. A shaker (SL-0505 in Fig. 14) vibrates the disk with the ten piezoelectric elements. The shaker is driven by an ac power supply (APD-050FCA in Fig. 14). Fig. 15 shows the size of the ten piezoelectric elements. The all area is 2.55×10^4 mm^2.

A. Numerical and Experimental Results

Fig. 16 describes the numerical results of the conventional circuit (without the resonator) and the proposed circuit (with the resonator) with DB, VD, and BC. Table III lists the

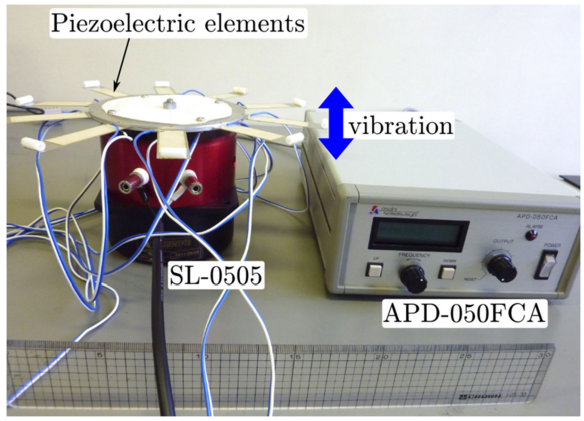

Fig. 14. Photograph of the vibration generator with piezoelectric elements.

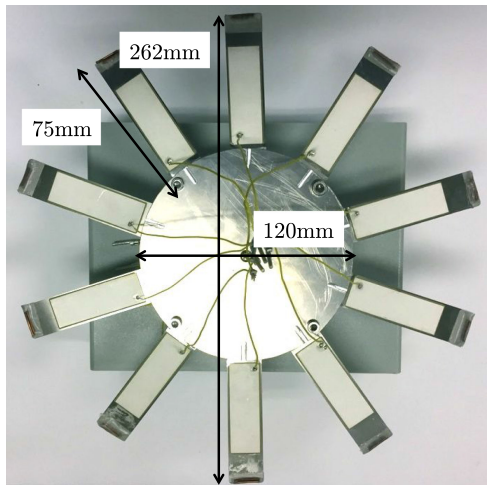

Fig. 15. Size of ten piezoelectric elements.

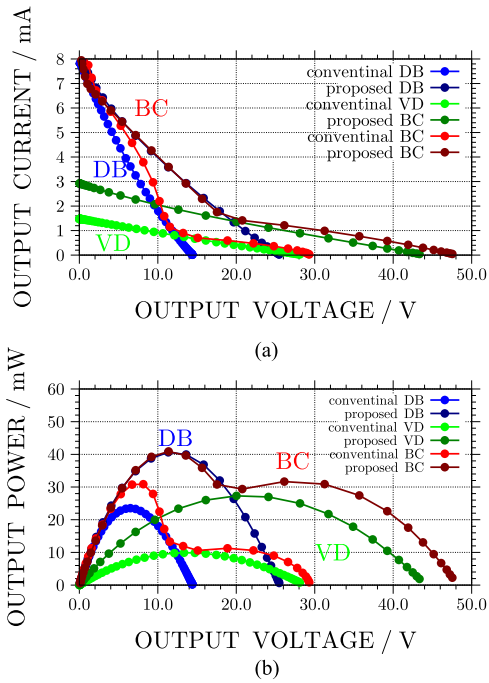

Fig. 16. Numerical results of I–V and P–V output characteristics in the conventional and proposed circuits with DB, VD, and BC. (a) I–V. (b) P–V.

TABLE III
MAXIMUM OUTPUT POWER EVERY CIRCUIT

	w/o Resonator	w/ Resonator
DB	23.5 mW	40.6 mW
VD	9.9 mW	27.3 mW
BC	30.9 mW	40.9 mW

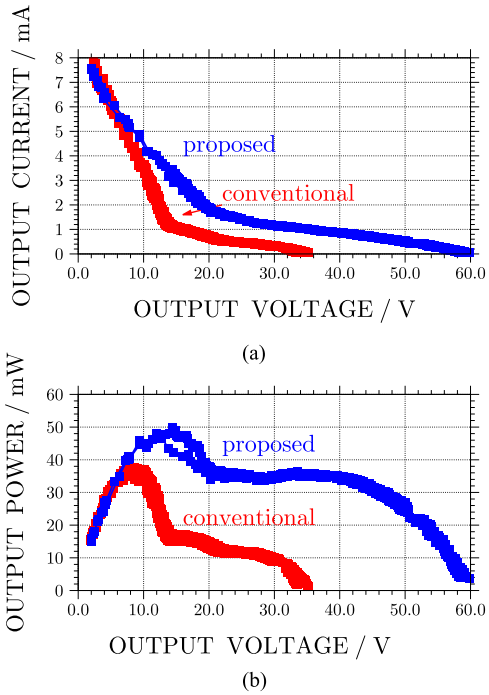

Fig. 17. Experimental results of I–V and P–V characteristics in the conventional and proposed circuits. Passive rectifier is BC. (a) I–V. (b) P–V.

maximum output power every circuit. The output characteristics of the proposed circuit are compared with the conventional circuit with BC. The maximum output voltage of the proposed circuit is 1.6 times as high as the conventional circuit, and the maximum output power of the proposed circuit is 1.35 times as large as the conventional circuit. In the low-voltage region, the output power is improved. Therefore, the vibration generators may be used for many systems. In contrast, in the high-voltage region, because the output voltage and power are improved, the vibration generators are able to maintain high power. Therefore, vibration generators may be used for many devices. For these reasons, the proposed circuit improves the output voltage and power, and vibration generators are expected to be increasingly used in the future for devices and systems.

The BC results in Fig. 16 have dips for both conventional and the proposed one. This shape is the output characteristic of the BC. In Fig. 8, BC resembles DB in the low voltage and VD in the high voltage because BC has two operation modes in Figs. 11 and 12. Therefore, the BC results in Fig. 16 have dips at the switching point.

Next, Fig. 17 describes the experimental results in this system. The results show the I–V and P–V characteristics in the conventional and proposed circuits. The maximum output voltage and power of the proposed circuit is higher than those of the

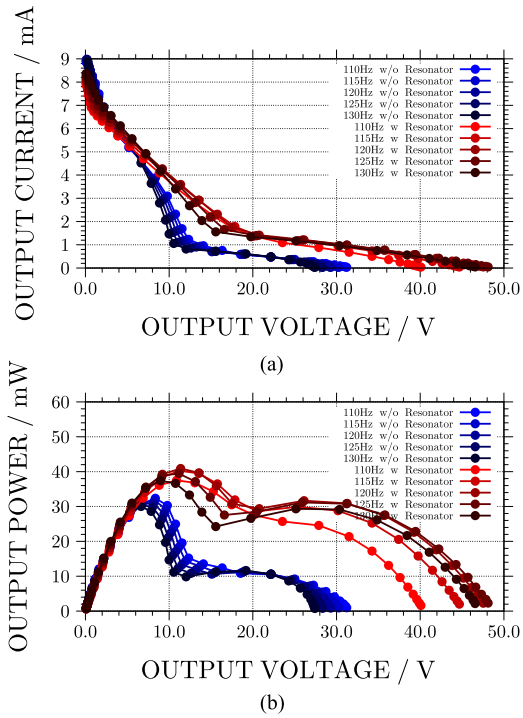

Fig. 18. Numerical results of I–V and P–V output characteristics around resonance frequency: from 110 to 130 Hz. (a) I–V. (b) P–V.

conventional circuit. The LC resonance improves the output voltage and power. In addition, Fig. 16 qualitatively matches those results.

B. Frequency Analysis Based on Numerical Results

This section analyzes the output characteristics around the resonance frequency. Fig. 18 describes the numerical results of the conventional circuit (without the resonator) and the proposed circuit (with the resonator) in Fig. 13. The vibration frequency changes from 110 to 130 Hz. From Fig. 18, the maximum output power changes by the vibration frequency and peaks at 120 Hz. In addition, the proposed circuit is not significantly affected by the frequency change around the resonance frequency.

As the results, the frequency lift affects the output power from vibration generators. Therefore, the C_{A} needs to adjust the LC resonant frequency for using the proposed resonator.

VI. SUMMARY

This paper has investigated the improvement in output characteristics obtained by using all passive devices, which are the inductors, capacitors, and diodes, with regards to the resonator and the rectifier. The proposed resonator used the LC resonance and equivalently reduced the internal capacitor of the vibration generators. In addition, the BC matches the vibration generators. The numerical and experimental results showed the effect of the LC resonance and the rectifier in improving the output characteristics in vibration generators.

In this paper, the novelty is to use electronic resonance in the vibration generators consisted of the piezoelectric elements. In

addition, the results in this paper contribute the numerical and experimental verifications of the proposed method.

ACKNOWLEDGEMENTS

The author would like to thank Mr. T. Sakabe for launching his early research and Ms. K. Kondo for calculating additional numerical results. The author would also like to thank Prof. M. Michihira and Prof. S.-i. Motegi for their fruitful comments and discussions.

REFERENCES

[1] L. Mateu, M. Echeto, and F. de Borja, "Review of energy harvesting techniques and applications for microelectronics," *Proc. SPIE*, vol. 5837, pp. 359–373, 2005.

[2] P. Spies, M. Pollak, and L. Mateu, *Handbook of Energy Harvesting Power Supplies and Applications*, 1st ed. Singapore: Pan Stanford, 2015, ch. 1.

[3] P. Glynne-Jones, S. P. Beeby, and N. M. White, "Towards a piezoelectric vibration-powered microgenerator," *IEE Proc.-Sci., Meas. Technol.*, vol. 148, no. 2, pp. 68–72, 2001.

[4] A. Erturk and J. Inman, "An experimentally validated bimorph cantilever model for piezoelectric energy harvesting from base excitations," *Smart Mater. Struct.*, vol. 18, no. 2, 2009, Art. no. 025009.

[5] H. S. Kim, J. Kim, and J. Kim, "A review of piezoelectric energy harvesting based on vibration," *Int. J. Precision Eng. Manuf.*, vol. 12, no. 6, pp. 1129–1141, 2011.

[6] C. B. Williams and R. B. Yates, "Analysis of a micro-electric generator for microsystems," *Sens. Actuators A, Phys.*, vol. 52, no. 1–3, pp. 8–11, 1906.

[7] F. Lu, H. P. Lee, and S. P. Lim, "Modeling and analysis of micro piezoelectric power generators for micro-electromechanical-systems applications," *Smart Mater. Struct.*, vol. 13, no. 1, pp. 57–63, 2003.

[8] P. Becker, B. Folkmer, and Y. Manoli, "The hybrid vibration generator, a new approach for a high efficiency energy scavenger," *in Proc. Int. Workshop Micro Nanotechnol. Power Gener. Energy Convers. Appl.*, Washington, DC, USA, 2009, pp. 439–442.

[9] L. Costanzo, A. Lo Schiavo, and M. Vitelli, "Power maximization from resonant electromagnetic vibration harvesters feeding bridge rectifiers," *Int. J. Circuit Theory Appl.*, 2018, to be published.

[10] M. Minami, T. Sakabe, S. Motegi, and M. Michihira, "Improvement in output power of vibration generators based on piezoelectric elements using passive devices (in Japanese)," *IEEJ Trans. Ind. Appl.*, vol. 137, no. 12, pp. 918–923, 2017.

[11] D. Kwon and G. A. Rincon-Mora, "A rectifier-free piezoelectric energy harvester circuit," in *Proc. IEEE Int. Symp. Circuits Syst.*, 2009, pp. 1085–1088.

[12] Y. K. Ramadass and A. P. Chandrakasan, "An efficient piezoelectric energy harvesting interface circuit using a bias-flip rectifier and shared inductor," *IEEE J. Solid-State Circuits*, vol. 45, no. 1, pp. 189–204, Jan. 2010.

[13] C. Peters, J. Handwerker, D. Maurath, and Y. Manoli, "A sub-500 MV highly efficient active rectifier for energy harvesting applications," *IEEE Trans. Circuits Syst. I, Reg. Papers*, vol. 58, no. 7, pp. 1542–1550, Jul. 2011.

[14] S. Hashimoto *et al.*, "Multi-mode vibration-based power generation for automobiles," in *Proc. Ind. Appl. Soc. Annu. Meeting*, 2012.

[15] H. A. Sodano, D. J. Inman, and G. Park, "A review of power harvesting from vibration using piezoelectric materials," *Shock Vib. Dig.*, vol. 36, no. 3, pp. 197–205, 2004.

[16] S. Roundy and P. K. Wright, "A piezoelectric vibration based generator for wireless electronics," *Inst. Phys. Publ. Smart Mater. Struct.*, vol. 13, pp. 1131–1142, 2004.

[17] N. Mohan, T. M. Undeland, and W. P. Robbins, *Power Electronics: Converters, Applications, and Design*, 3rd ed. Hoboken, NJ, USA: Wiley, 2003, ch. 6.

[18] J. G. Kassakian, M. F. Schlecht, and G. C. Verghese, *Principles of Power Electronics*, 1st ed. Reading, MA, USA: Addison-Wesley, 1991, ch. 4.

[19] K. Fujiwara and H. Nomura, "A new operating principle of voltage-doubler diode rectifiers to meet the harmonic guide lines (in Japanese)," *IEEJ Trans. Ind. Appl.*, vol. 119, no. 1, pp. 103–108, 2008.

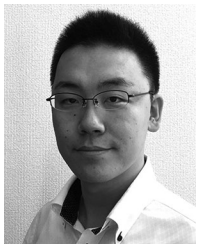

Masataka Minami was born on November 9, 1985, in Fukuoka, Japan. He received the bachelor's, master's, and Ph.D. degrees from Kyoto University, Kyoto, Japan, in 2008, 2010, and 2013, respectively.

In 2013, he joined the Department of Electrical Engineering, the Kobe City College of Technology, Kobe, Japan, where he is currently an Associate Professor. From April 2018 to March 2019, he will be an Academic Visitor with the School of Engineering, Ecole Polytechnique Federale de Lausanne, Lausanne, Switzerland. His research interests include rectifiers, dc/dc converters, inverters, power systems engineering, and control applications.

Dr. Minami was a recipient of the IEEJ Industry Applications Society Excellent Presentation Award in 2017. He is a member of the Institute of Electrical Engineers of Japan, the Institute of Electronics, Information and Communication Engineers, and Institute of System, Control and Information Engineers.